

Article

A Methodological Study on the Design Defending Baffles Based on Mangrove Bionics

Yu-Zhang Bi ^{1,2,†} , Xin-Yi Wang ^{3,†}, Dong-Po Wang ^{1,*} , Zhuo-Fan Li ², Marco Lovati ^{1,4} and Bei Zhang ^{5,6,7} 

¹ State Key Laboratory of Geohazard Prevention and Geoenvironment Protection, Chengdu University of Technology, Chengdu 610059, China; byz690@yeah.net (Y.-Z.B.); marco.lovati@eurac.edu (M.L.)

² Institute of Geotechnical Engineering, Southeast University, Nanjing 210096, China; geladun@163.com

³ School of Design, Hong Kong Polytechnic University, Hong Kong 999077, China; 22047408g@connect.polyu.hk

⁴ Department of Built Environment, Aalto University, Otakaari 1B, 11000 Espoo, Finland

⁵ College of Geological Engineering and Geomatics, Chang'an University, Xi'an 710054, China; beizhang@chd.edu.cn

⁶ Key Laboratory of Western China's Mineral Resources and Geological Engineering, Ministry of Education, Chang'an University, Xi'an 710054, China

⁷ Department of Geotechnical Engineering, College of Civil Engineering, Tongji University, Shanghai 200092, China

* Correspondence: wangdongpo2014@cdut.edu.cn

† These authors contributed equally to this work.

Abstract: In terms of the failure of giving considerations to both aesthetic ornamental and low-carbon function for the current disaster prevention and mitigation engineering. This study proposes the debris-disaster prevention baffles applicable to natural scenic areas which designed based on mangroves properties, to solve this problem by adopting bionic design method. The research methodology is as follows: (1) To propose a *Six Elements and Ten Steps* Design Method for extracting the critical bionic elements of mangrove plants that contributes to the prevention of winds and waves. (2) To construct a decision objective model based on the Analytic Hierarchy Process method (AHP). Prioritize the critical bionic design elements and build a geometric structure model. (3) To compare the disaster mitigation performance through numerical simulations, and thus select an optimal one for further studies. (4) To design the final disaster prevention product based on the above theoretical guidance, low-carbon concept, efficient protection orientation, and environment-friendly principles. This study indicates that the use of bionic design satisfies aesthetic ornamental, and low-carbon demands. The appliance of AHP avoids subjective one-sidedness in design process when considering the priority of bionic elements. The numerical simulation experiments adopted in this study aim to compare the blocking effect of different baffle models and achieve the optimization the performance in disaster prevention of traditional baffle groups. In this study, the bionic product design methodology is adopted for baffle design to solve existing aesthetic and environmental problems. The particle accumulation mass after the new baffles can be effectively reduced by 2–3 times compared to the traditional baffles. Furthermore, the new baffle is more aesthetically pleasing than the traditional ones.

Keywords: mangroves; bionics; disaster prevention and mitigation; product design; discrete element method



Citation: Bi, Y.-Z.; Wang, X.-Y.; Wang, D.-P.; Li, Z.-F.; Lovati, M.; Zhang, B. A Methodological Study on the Design Defending Baffles Based on Mangrove Bionics. *Buildings* **2023**, *13*, 310. <https://doi.org/10.3390/buildings13020310>

Academic Editors: Wei Wang, Xianwen Huang, Peiyuan Chen, Aizhao Zhou, Shaoyun Pu and Wei Duan

Received: 13 November 2022

Revised: 8 December 2022

Accepted: 14 December 2022

Published: 20 January 2023



Copyright: © 2023 by the authors. Licensee MDPI, Basel, Switzerland. This article is an open access article distributed under the terms and conditions of the Creative Commons Attribution (CC BY) license (<https://creativecommons.org/licenses/by/4.0/>).

1. Introduction

1.1. Mangroves and Their Ecological Efficacies

Mangroves, the tidal wetland woody biome that grows on the mudflats in the border zone between land and sea, constitutes a unique transitional ecosystem. Mangroves consist of evergreen shrubs and arbors, herbaceous plants and liane with air or prop roots [1]. Figure 1a,b are mangroves and their habitats, respectively. Mangroves have a high ecological value for their efficacy in the protection of winds waves, and the shores as well as deposition promotion and seawater purification [2]. In 1986, the 294 out of

the 398 km long seawall in Hepu County was damaged by storm tide off the coast of Guangxi, China. However, those covered by mangroves were more likely to survive the big waves [3]. Figure 1c shows 2004 Indian Ocean tsunami. The 2004 Indian Ocean Tsunami struck 12 countries and killed 230,000 people. However, 172 families in the Indian fishing village of Singarathop just on the coast miraculously survived the catastrophe thanks to the dense mangroves growing on the shore (Figure 1d) [4]. In 2012 the Cambridge University Coastal Research Group found [5] that there is a decrease in the height of the waves when they pass through the mangroves. In a mangrove forest of 500 m in width, wave heights would be reduced by between 50% and 99%. This study demonstrates the effectiveness of mangroves in protecting the shore against winds and waves.

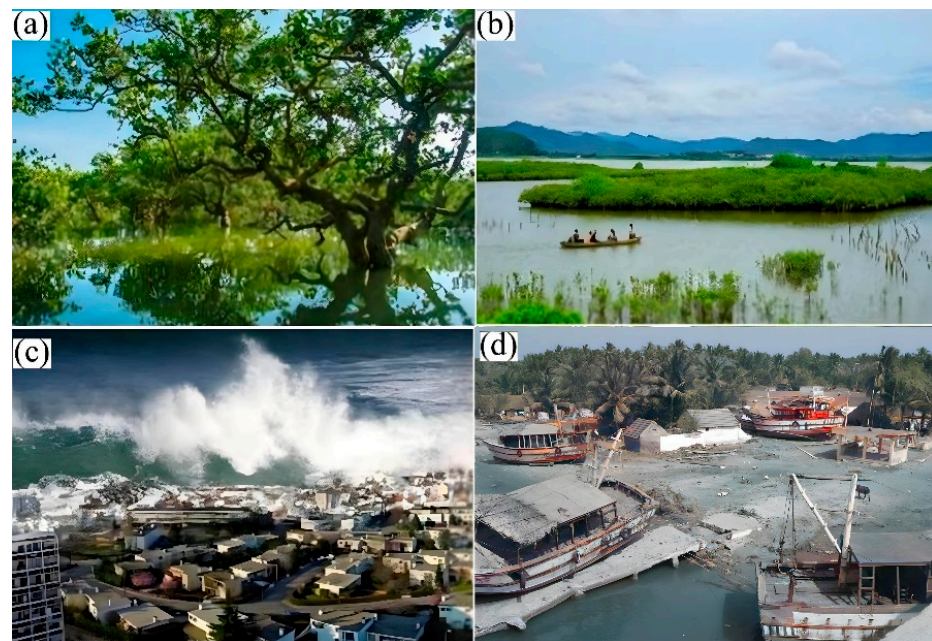


Figure 1. Examples of mangroves and their disaster preparedness: (a) mangrove plants (<http://www.forestry.gov.cn/main/416/20201209/094618527742186.html> (accessed on 9 December 2020)), (b) mangrove habitat (http://k.sina.com.cn/article_5787187353_158f1789902000iq61.html (accessed on 19 November 2018)), (c) the 2004 Indian Ocean tsunami (https://www.sohu.com/a/205476684_644208 (accessed on 20 November 2017)), and (d) Singarathop fishing village [4].

Mangroves generally grow in coastal areas and cannot alive far away from the sea water. They cannot grow inland in mountainous areas. The main factors which affect the distribution and growth of the plants are the mangrove’s adaptability to the chemical environment, the soil composition and the sea salinity. As the mangroves cannot grow inland directly for engineering use, the mangrove bionics design should be used in engineering structures to improve the performance.

1.2. Baffle Group Structure Based on Debris Flow Control

As a common geological disaster, debris flow brings great economic losses to human society. Debris flow has a higher volumetric weight than water flow, and its fluid dual structure with solids (rocks and soils) is characterized by high kinetic energy and high impact force [6–8]. The intense scouring generated by debris flow can lead to drastic abrasion of the ditch bed and collapse of the bank. This can easily lead to a vicious circle, where the collapse will be adding to the scale and the frequency of the flaws. In addition, the flaws will be a serious threat to the towns, roads, water channels, farmlands, forests and other infrastructures [9], severely influencing the people’s lives [10,11]. Therefore, it is of great socio-economic and ecological significance to design and produce a management engineering product that can effectively mitigate debris flow.

Regulation projects on debris flows mainly includes interception projects, water storage projects, drainage works, and ecological engineering [12]. Interception and storage projects can significantly reduce the debris flow hazard by intercepting the solids in the flow by consolidating the loose solids in it. Among the many engineering structures, the baffles group is a fundamental and widely used one. [13–16]. Figure 2a,b shows that an array of baffles is a structure in which multiple baffles are arranged and set according to some specific rules [14,16]. The use of the low profile reinforced concrete baffles can slow down or regulate the flow of debris by increasing the roughness of the ditch bed of the debris flow [17].

Some nature reserves and tourist attractions in China have complex natural conditions and often have the potential for frequent debris flows [18] (Figure 2c,d). The current baffle groups used for the prevention of mud flows are generally simple and rough in appearance, and the root columns are arranged in a dull manner. This severely contrast with the beauty of the natural ecological environment of nature reserves and tourist attractions [19]. Furthermore, the traditional design of the baffles group mainly focused on the efficient protection rather than consider both the efficient protection, low-carbon and environmental-friendly concept. Another problem is that the existing baffles are mainly made of cement, which can be highly alkaline and generally leads to more carbon emissions and pollution problems. Therefore, the innovative baffle group structure needs to pay special attention to the ornamental and aesthetic aspects of the design of debris flow prevention and mitigation engineering, so that the design of disaster prevention and mitigation engineering and nature can achieve harmonious integration and unity.



Figure 2. The existing baffles and mudslide hazards in natural landscapes: (a) array of baffles in Hong Kong [20], (b) array of baffles in mainland China [21], (c) damage to the landscape from the Jiuzhaigou mudslide disaster (<https://www.jiuzhai.com/news/scenic-news/6686-2019-07-22-10-37-47> (accessed on 22 July 2019)), and (d) damage to roads from the Jiuzhaigou mudslide disaster (<http://news.huaxi100.com/show-226-799121-1.html> (accessed on 23 July 2016)).

1.3. Current Status of Bionic Product Design Research

1.3.1. Overview of Bionics

The concept of bionics was originally introduced by Steele at the first World Congress of bionics in the 1960s [22]. Bionics is the science of constructing technological systems that

mimic the principles of biological systems. It is used to make artificial technical systems with characteristics of biological systems or similar features. In this scenario, bionics represents an alternative tool for designers. It is a multidisciplinary science that researches the principles, properties and mechanisms of natural systems (structures, processes, functions, organizations and interrelations), with the aim of applying them in the development of new products or solving technical problems that may arise during project-phase [23].

After billions of years of evolution and natural selection, nature has developed optimal morphological structures, efficient material metabolism recycling systems under precise control and regulation. Bionics provides new design ideas, working codes, and systems for various research fields based on the combination of engineering technology and the study of the structure, traits, principles, behavior, and interactions of the natural biological systems. Bionics in the research field includes structural bionics, morphological bionics, mechanical bionics, mimetic bionics, etc. [24].

1.3.2. The Application of Bionics in Product Design

Bionics-based product design is generally a creative approach to make such products more effective by combining the functional characteristics of the design with the structure, form, texture, and function of certain plants or animals [25].

Bionic product design is divided into four main types: morphological bionic, material bionic, structural bionic, and functional bionic [26]. Figure 3 is the summary the types their features. Structural bionic and functional bionic are especially important in engineering. Structural biomimetic design focuses on the analysis of the structural characteristics of natural organisms. The use of this structure can achieve the functional needs as well as the aesthetically pleasing at the same time. Functional bionic design studies the potentially applicable objective principles of natural microorganisms to gain inspiration for optimizing the products' performance.

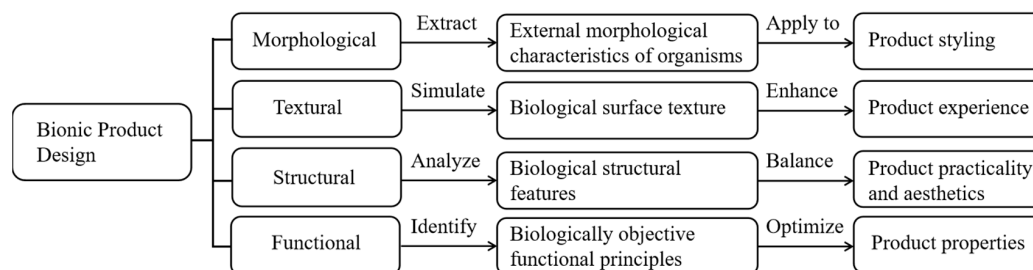


Figure 3. Summary and analysis of bionic design types and characteristics.

Bionic product design covers various fields such as daily appliances, commodity packaging, office appliances, sports equipment, architectural space, and mechanical equipment. Nendo's Peggy money jar is a vivid example of functional bionic design [27], The designer takes the characteristics of a pig and make it into a jar in the shape of a pig's snout (Figure 4a). MUJI designer (Naoto Fukasawa) referred to material texture bionics [28] and mimic the color and texture of fruits (bananas, strawberries, and kiwis) to create a more interesting juice box (see Figure 4b). The pangolin backpack [29] designed by Uriel Serrano is a structural bionic design with a shell that mimics the structure of the pangolin's keratin scales. The pangolin chair also refers to the shape of the pangolin in order to better prevent the user away from outside noise and meanwhile make it easier to be stored and folded (Figure 4c). The German company Festo has optimized its robotic arms on their telescoping and flexibility and enables them to perform better when carrying heavy loads by drawing on the structure of an elephant's trunk [30] (see Figure 4d). The skull structure of the bird was found to be very light but highly impact-resistant. Thus, it was used in energy-efficient bio-building materials [31] (see Figure 4e). The LEX wearable bionic chair pays extra attention to the skeletal structure [32] to meet the user's need to be able to sit down at any times (see Figure 4f).



Figure 4. The application of bionics in product design, (a) Peggy money jar (<https://mp.weixin.qq.com/s/Utcnq2I7jw1DGjhA7eHc-Q> (accessed on 5 August 2018)), (b) MUJI juice box (<https://mp.weixin.qq.com/s/cBDQjeHmo2WESun052nQlw> (accessed on 9 June 2020)), (c) pangolin backpack (<https://mp.weixin.qq.com/s/zgvb2ORflXOgIw5Fo-1nOw> (accessed on 17 March 2015)), (d) Festo robotic arm (<https://mp.weixin.qq.com/s/wxKwO21wV4kp-oT2AZqB2w> (accessed on 12 September 2021)), (e) energy efficient biological building materials for the bionic bird skull structure (https://mp.weixin.qq.com/s/1qN4fwEtKdzyd2J67EZ_2A (accessed on 26 July 2016)), and (f) LEX wearable bionic chair (https://mp.weixin.qq.com/s/BNOTrEP_heiY-EWJEBfbGA (accessed on 7 December 2020))).

1.4. Overview of the Development of Bionic Product Design in Engineering

Bionics product design has a long history of research and application in the engineering field. The biological features are mainly extracted through four kinds of bionic designs: form bionic, material texture bionic, structure bionic and functional bionic design bionic. Moreover, the bionics product design has achieved major breakthroughs and effective innovations in various fields of engineering. At the end of the 20th century, it was found that the bullet locomotive “pushed” the air in front of the train driving through narrow lanes produced a sonic explosive effect, whose noise far exceeded environmental standards. To solve this problem, Japanese engineering designers modified the bullet-shaped nose of a train by mimicking the beak section of a kingfisher [33], resulting in a 10% increase in speed, a 15% reduction in power consumption, and a significant reduction in noise levels (see Figure 5a). In the early 21st century, the Osaka Institute of Technology in Japan designed a serrated needle tip that mimicked the mouthpiece of a mosquito. In contrast with conventional cylindrical syringes, the central needle tip is provided with two subtle outer jagged strips next to it, which can significantly reduce the pain of lancing into the human body [34]. This is due to the way that the mosquito’s mouth touches the human body allows it to touch as little as possible human skin nerves, thus reducing human pain (see Figure 5b). Omni-ID’s company has created radio frequency ID tags by mimicking the subtle laminar structure on the wings of a blue butterfly. In addition, a series of exquisite metal sheets were used to gather and change the incoming radio waves and reflect clear signals for remote identification [35]. They chose to do that for the laminate structure on the wings of this butterfly reflects sunlight from different angles and creates dazzling colors (Figure 5c). In 2020, Ben-Gurion University in Israel developed and designed AmphiSTAR. This new high-speed amphibious robot enables high-speed swimming and running on the water surface and crawling on the ground through a bionic snake monster lizard [36] equipped with four propellers and a pair of buoyancy tanks on the bottom. Since the snake monster lizard has slender toes and covers scales under the bottom of the feet, when

the scales contact with the water, the air bubbles will not break the balance of the water surface tension, it will still run at high speed (see Figure 5d). In 2022, Mercedes launched the bionic concept car called “Bionic” [37] with the growth principle of trees and bones to reduce the materials of small stressed parts. It further strengthens the materials of high load parts until the body weight is reduced by about 30%. Meanwhile, it maintains stability, crash resistance and driving experience. Both trees and bones have light but high strength characteristics. The trees increase the weight at important stress points, while the bones remove the necessary material without needed, using as little material as possible to achieve maximum robustness (see Figure 5e).

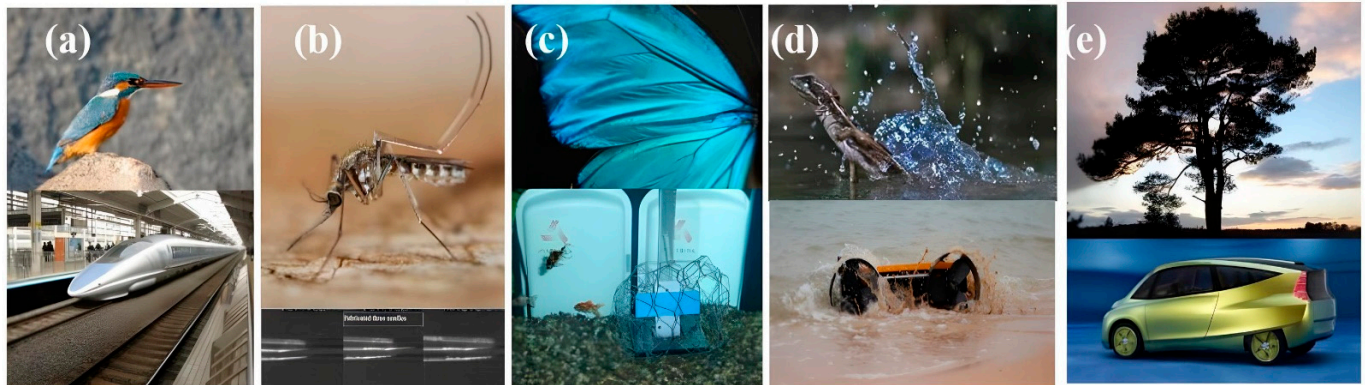


Figure 5. Application of bionics product design in the engineering field: (a) the bionic kingfisher beak train head, (https://mp.weixin.qq.com/s/1qN4fwEtKdzyd2J67EZ_2A (accessed on 26 July 2016)), (b) the zig-toothed tip of a bionic mosquito mouthpiece (<http://www.sinoca.com/news/tech/2011-08-24/158796.html> (accessed on 24 August 2011)), (c) the Omni-ID remote identification system (<http://www.sinoca.com/news/tech/2011-08-24/158796.html> (accessed on 24 August 2011)), (d) the new high-speed amphibious robot AmphiSTAR (<http://www.sinoca.com/news/tech/2011-08-24/158796.html> (accessed on 24 August 2011)), (e) the “Bionic” concept car launched by Mercedes (<http://www.sinoca.com/news/tech/2011-08-24/158796.html> (accessed on 24 August 2011)).

Currently, bionics-based product design in the engineering field mainly covers transportation engineering, medical engineering, electrical engineering, mechanical engineering, and automotive engineering, but has seldom been applied to the field of geotechnical engineering and thus a systematic study into this new field is necessary. The scientific research steps of this paper are as follows (see Figure 6): firstly, literature research is conducted to build the relationship between the mangroves and baffles. Secondly, the Analytic Hierarchy Process method (AHP) is adopted to unveil the key bionics design parameter. Thirdly, the numerical studies are conducted to determine the best case of engineering design. Lastly, the bionics design is conducted to make the baffles more ornamentally aesthetic. The main research methods are as follows: (1) this study will first propose a *Six Elements and Ten Steps* Design Method for extracting the critical bionic elements of mangrove plants. (2) We will construct a decision objective model based on the Analytic Hierarchy Process method (AHP). Prioritize the critical bionic design elements and build a geometric structure model. (3) We will compare the disaster mitigation performance through numerical simulations and finally provide a practical solution for designing disaster prevention products applicable to natural scenic areas.

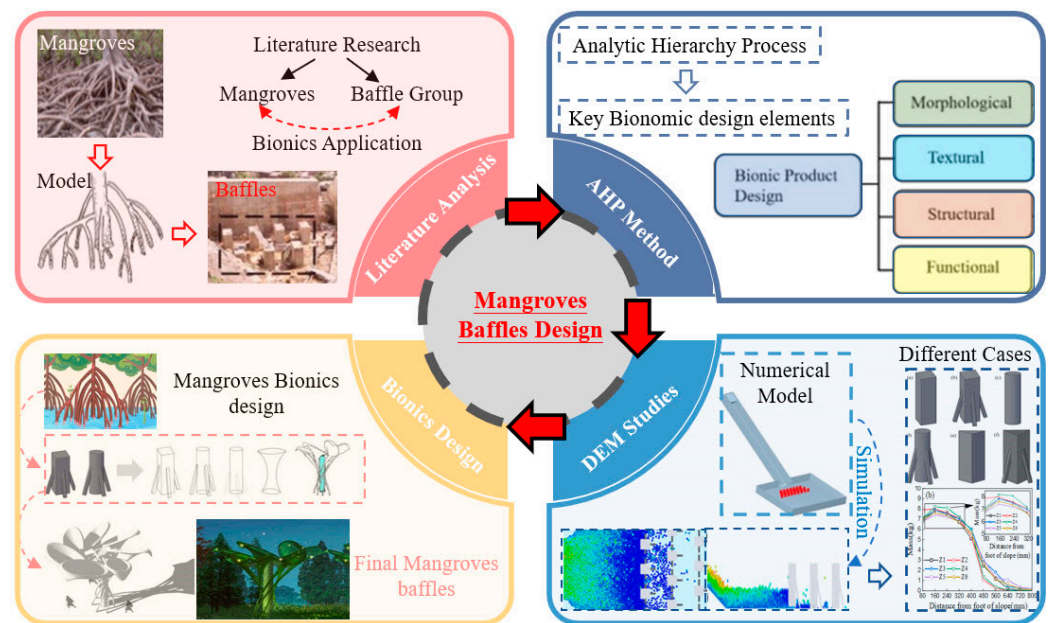


Figure 6. The scientific research steps of this study.

2. Research Methodology and Design Process

2.1. Design Concept of Bionic Product

2.1.1. Overview of Six Elements and Ten Steps Biotic Design

The biotic design originated from the inspiration of natural organisms. It achieves innovation through the extraction, analysis and imitation of a series of features such as the structure, function and form of living organisms.

The *Six Elements and Ten Steps* design method, based on the biotic design theory, begins with a detailed analysis of the six elements of the bionic prototype: form, structure, texture, color, function, and system, which aims to explore the core reasons for the realization of a specific goals of the bionic prototype and extracts the key features. *The Six Elements and Ten Steps* represents a widely applied design methodology and reflects a symbiotic and harmonious relationship between product design and bionic design. The design process is illustrated in Figure 7, the six elements are form, structure, texture, color, function, and system, and the overall design process is divided into the following ten steps:

- (1) Clarify the demand for the optimization of the product. Analyze the current state of research according to the subject, explore the problems of similar products, and clarify the specific needs for product performance optimization.
- (2) Compare and analyze similar bionic prototypes. Collect a variety of creatures and classify them based on the bionic design concept.
- (3) Select the best prototype for bionic design. Compare the alternative bionic prototypes by listing the similarities associated with the creatures and finally select the best match for the optimal performance.
- (4) Dismantle the six core elements of the prototype. Dissect in detail the six core elements of the biomimetic object, namely form, structure, texture, color, function, and system.
- (5) Explore the reasons for achieving the performance goals. Investigate and explain the core elements and reasons for achieving the goals based on the analysis of the six elements of the biomimetic prototype.
- (6) Establish a chain of element-performance relationships. Establishing relationships between elements and target performance in balance regulation, immune resistance, supply support, information exchange, etc.
- (7) Extract critical features of relevant elements. Extract the elements with the highest weight by the analytic hierarchy process (AHP), and further conclude the bionic key features, and construct several geometric structure models.

- (8) Conduct simulation experiments to evaluate the effect of the model. Test the performance of the geometrical structural model through numerical simulation and other scientific experimental methods. Compare and the experimental results, and select the best structural model from them.
- (9) Adjust design elements according to the project. Transform the design elements into the shape of the product with the consideration on the environmental integration, scientific feasibility, artistic aesthetics, functional orientation and other design principles
- (10) Complete the target performance-oriented scheme. Use design tools to establish product models and optimize the design concepts, structural shapes, colors and materials, functional applications, market values, and other aspects for the final design.

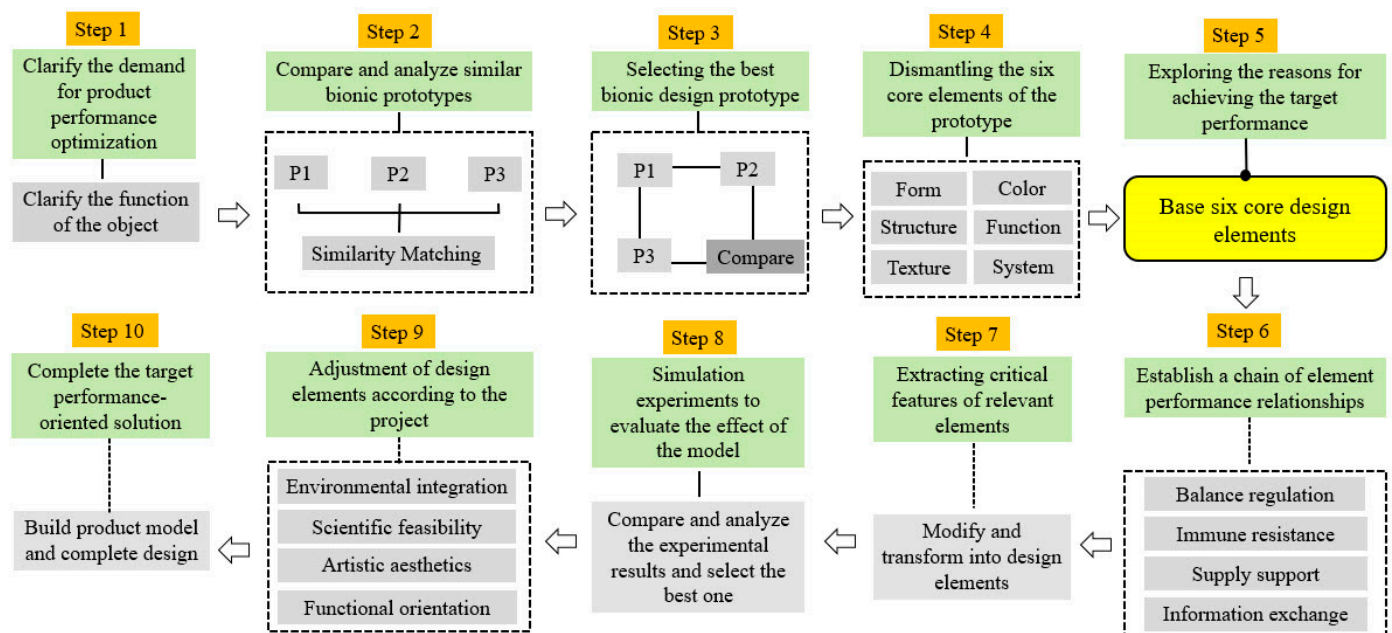


Figure 7. Six Elements and Ten Steps system bionic design method.

2.1.2. Mangroves and Bionic Design

Considering the special growing conditions of mangroves, though, the trees have the ability to prevent the winds and waves, they can only be planted in the mudflats in the border zone between land and sea. Though the mangrove has the potential to prevent the winds and waves, they are suitable for most seashores. If the existing baffle groups can be optimized by the bionic use of mangroves, the function on wind and wave prevention of this plant may be applied in nature reserves and tourist attractions on large scales, thus effectively prevent debris flows and add to the security.

At the same time, the mangrove forest is of great ornamental values and this can be a solution to the problem of appearance of the current baffles. This cooperation may achieve the harmony between the protection of the natural reserves and the prevention of natural disasters.

2.2. Analytic Hierarchy Process Method

2.2.1. Overview of Analytic Hierarchy Process

Analytic Hierarchy Process (AHP), proposed by Thomas L. Saaty, an operations researcher, in the early 1970s is a practical and effective multi-criteria decision-making method that can express subjective judgments in quantitative forms. It combines qualitative words with quantitative numbers, and conducts systematic and modeled analysis of samples through mathematical models in order to effectively avoid the subjective and one-sided decisions in the analysis of complex problems.

2.2.2. Bionic Design and Hierarchical Analysis

The bionic design is supposed to analyze and extract diverse design elements from the bionic prototype's morphology, structure, texture, color, to the function, and system. The analytic hierarchy process is just suitable for analyzing multiple elements. Providing the wide use of bionics in the field of design and the need for further study, a new type of the analytic hierarchy Process (AHP) suitable for bionics is introduced. In order to acquire the exact bionic design elements, first, it is to analyze mangrove forest from morphology, color, structure, texture, function and system for the core reasons of the effective prevention and conclude the key points. Next, researchers will figure out the weight values of all bionic design elements, listed them in descending orders and discover the scientific and valuable results, as shown in Figure 8.

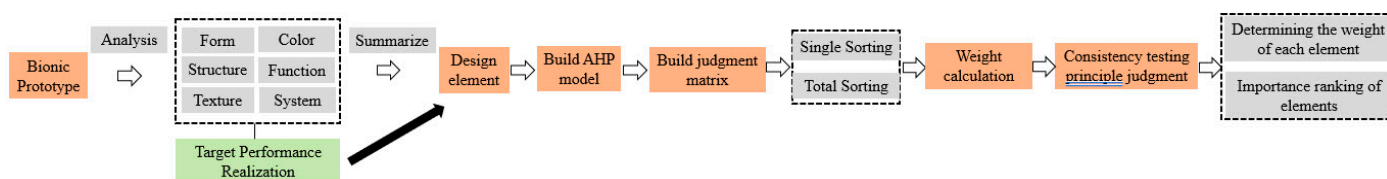


Figure 8. AHP method suitable to bionics.

2.3. Analysis of the Design Process

The innovation of the structural products for disaster prevention and mitigation lies in the “Six Elements and Ten Steps”. The key elements of the preventing design is extracted and transformed from the form, structure, texture and function of the mangroves. The AHP is used to construct the hierarchical structure model, calculate the weight of the design elements, select and analyses the object according to the calculation and decide on the core design elements, and build the geometric bionic structure model. Next, pick the best one through the numerical simulation experiment and comparative analysis, transform it into the model of the product, and finally complete the design scheme. It is to innovate the design mode, improve the design efficiency, optimize the product performance, and maximize the product engineering efficacy. The design process is shown in Figure 9. It consists of the following seven steps:

- (1) Explore the core reasons for mangroves' wind and wave protection function and extract the key features by analyzing the mangroves from morphology, structure, texture, function and system aspects.
- (2) Make an in-depth analysis of key features. clarify the relationship between the prototype features and the function of wind and wave protection, and transform them into clear bionic design elements.
- (3) Apply the AHP to transform the mangrove bionic design elements into a recursive hierarchical model. A judgment matrix is used to quantify the design elements with mathematical methods. It selects the key factors determining mangroves' wind and wave protection performance.
- (4) Arrange the elements of the biotic design in descending order and conduct proper analysis.
- (5) Make several prototypes of the core structure of the product design based on the core features and design elements of the bionic design.
- (6) Compare the blocking effect of different structural models and pick the best structural model by the comparative analysis of the results of numerical simulation for the scientific feasibility of disaster prevention and mitigation performance.
- (7) Modify and beautify the best model and form the final target performance-oriented bionic design scheme with the considerations on the design principles of environmental integration, scientific feasibility, artistic aesthetics, and practical orientation.

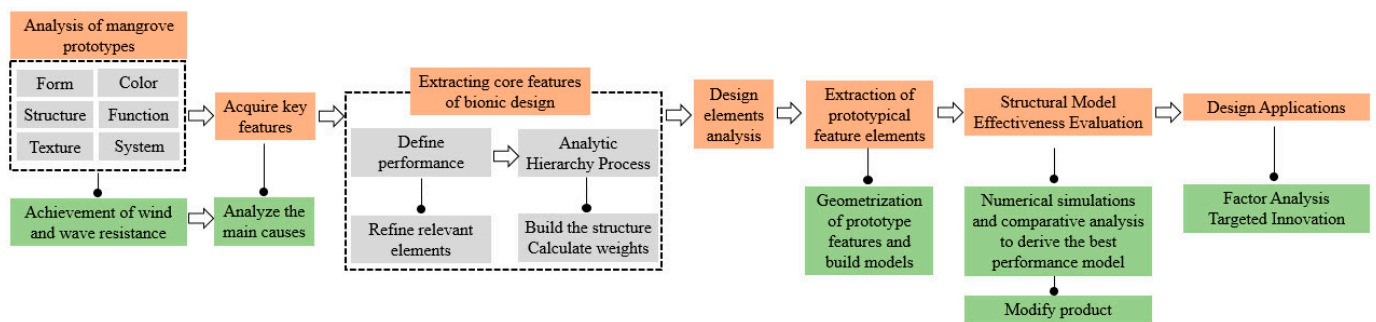


Figure 9. The design flow chart of disaster prevention and mitigation structure products based on mangrove bionics.

3. Design Process

3.1. Selection of Mangrove Characteristics

Based on the “six elements and ten steps” systematic principles on bionic design, the six elements (morphology, structure, texture, color, function, and system) of mangrove forests were selected to analyze the core reasons for wind and wave protection and to extract the critical features for disaster migration.

3.1.1. Analysis of “Six Elements” of Mangroves

- (1) Morphologically, the gently sloping terrain of the tidal zone determines that the inundation depth of mangrove plants varies. Mangrove plants are often monodominant community with a simple spatial structure and a green or gray-green to silver-grey appearance, and the height of the forest span from 1 m to 30 m. In addition, the the aerial root and prop root of mangrove plants are morphologically unique. Due to the flush of the tides and the lack of air, the plants has developed different types of aerial roots, prop roots, and respiratory roots, such as plate-like roots, finger-like roots, knee-shaped roots, and snake-shaped creeping roots.
- (2) Structurally, roots, trunks, branches, and leaves constitutes the main structures of mangrove plants. The root system is divided into respiratory, prop and aerial roots, and enables the mangroves to stand stable in the mudflat. The roots of mangrove plants tend to grow close to the surface. They are either horizontally distributed cable-like roots or surface roots exposed to the air. Most plate roots and arching prop roots growing from the branch trunks are embedded in the mudflats to enhance their capacity to keep the plant stable. Finger-like aerial roots are specially adapted to the mudflat environment. They grow from the roots and droop downward from the branches and expose to air on the beach floor. The shoot-like respiratory roots that wriggling across the ground, either in knee-shape or vertically upward, works well in oxygen intake and can be used for aeration at low tides or even when submerged. The large quantity of the far spread deep roots enables the mangrove plants stand firm and stable on the soft and drifting sandy mud.
- (3) In terms of texture, the bark and trunk of mangrove plants show the basic texture of shrubs.
- (4) In terms of color, the appearance of mangrove plants is green or gray-green to silver gray. Due to the mono-tannic acid contained, the plants can reddish-brown when oxidated, and that is the reason why it ofteh has a reddish-brown when being cut or felled, and this is also the reason how the name mangrove comes.
- (5) Functionally, the well-developed root system with a huge biomass has a series of functions such as respiration and the transmission of oxygen, as well as reducing the power of the waves. The aerial roots on the ground and the underground roots exchange the air with each other so that they do not become stuck and suffocated in the mud due to the lack of oxygen, ensuring the proper oxygen that meet the

respiratory needs of the mangrove plants. At the same time, the root system can fasten sediment in the mudflat and reduces the reflux rate of the silt.

- (6) Systematically, the aeration structure of the aerial roots enables the plants with strong permeability and ability to take in oxygen from the seawater. The rich tannis in the bark contributes to the infiltration and corrosion protection. The release of tannins in seawater can reduce the alkalinity of seawater. The leaves are succulent and thick, covered with a layer of wax to prevent water loss. They contain salt-retentive tissue, so that excess salt can be secreted through the salt glands.

3.1.2. Analysis of the Causes of Wind and Wave Protection in Mangroves

Based on the above analysis of the six elements, it can be concluded that the wind and wave protections are mainly related to the plants' morphology, structure, and system. The key features of morphology are a well-developed root system, dense canopy and monodominant community. The key features of structure are aerial roots, prop roots and respiratory roots. The key features of the system are aeration and water absorption systems, infiltration and antiseptic system and salt excretion system.

3.2. Prioritizing Analysis of Elements in Mangrove Bionomic Design

3.2.1. Calculation on the Index Weights of the Elements

According to the analysis above, the main indicators of mangrove bionic contain: morphology, structure, and system. According to the results of the feature analysis, the grade standard on mangrove bionic design is established, as shown in Table 1.

Table 1. The evaluation index of mangrove bionic design.

	First Level Indicators	Second Level Indicators
Mangrove bionic design element (U)	U1: Form	U11: Developed root system, U12: Monodominant Community, U13: Dense Canopy
	U2: Structure	U21: Prop roots, U22: Aerial roots, U23: Air root
	U3: System	U31: Aeration and Water Absorption Systems U32: Permeation and Corrosion Protection System, U33: Salt Excretion System

The method of questionnaire for experts is used to determine the weights of the above indicators. In this study, the weights of the secondary indicators were calculated as an example. Assuming that there are L experts invited to the evaluation according to Delphi Method. The ranking matrix is obtained based on the statistical results and is noted as,

$$A = (a_{xi})_{L \times M} (x = 1, 2, \dots, L, i = 1, 2, \dots, M)$$

The experts' scores will then be applied to the entropy theory for their entropy values. The specific steps are as follows:

- (1) Calculate the degree of subjective average recognition by the Degree of Membership Function:

$$b_{xi} = -\frac{\ln(h - a_{xi})}{\ln(h - 1)}, h = M + 2 \quad (1)$$

where the matrix of the degree is $B = (b_{xi})_{L \times M}$, where b_{xi} is the degree of a_{xi} , then the average recognition degree b_i of all experts for the indicator i is:

$$b_i = b_{1i} + b_{2i} + \dots b_{Li} / L \quad (2)$$

- (2) Define the degree of the recognition deficiency, denoted as Q_i :

$$Q_i = \frac{|\max(b_{1i}, b_{2i}, \dots, b_{Li}) - b_i + \min(b_{1i}, b_{2i}, \dots, b_{Li}) - b_i|}{2} \quad (3)$$

(3) The overall recognition of experts for each indicator is denoted as r_i , then:

$$r_i = b_i(1 - Q_i) \quad (4)$$

Next, the weight of the i th indicator in a specific level is:

$$w_i = \frac{r_i}{\sum_{i=1}^M r_i}, \omega_i > 0 (i = 1, 2, \dots, M) \quad (5)$$

According to the above theory, taking the mangrove bionic prototype in this study as an example, the weights of the secondary indicators in this study can be determined according to the experts' scores, as shown in Table 2.

Table 2. The weight of secondary indicators.

Second Level Indicators	Weight
U11: Developed root system	0.8
U12: Monodominant Community	0.1
U13: Dense Canopy	0.1
U21: Prop root	0.6
U22: Aerial roots	0.3
U23: Breathing root	0.1
U31: Aeration and water absorption systems	0.5
U2: Permeation and Corrosion Protection Systems	0.4
U33: Salt Excretion system	0.1

According to the above distribution of weight, all the secondary indicators can be divided into major, medium, and minor indicators, and the specific descriptions are shown in Table 3.

Table 3. The index and description of mangrove bionic design.

Element	Key Impact Indicators	Moderate Impact Indicators	Minor Impact Indicators
Form	Developed root system	Dense Canopy	Dense Canopy
Structure	Prop root	Aerial roots	Breathing root
System	Breathing and Absorption system	Permeation and Corrosion Protection Systems	Salt Excretion System

Table 4 shows the range of scores given according to the importance of each secondary indicator. The lower a indicator scores, the less important it is. In addition, the final score of the first-level indicators is calculated according to the weights of the second-level indicators. The formula for scoring the first-level indicators is shown as follows:

$$P = 0.8 \times p1 + 0.1 \times p2 + 0.1 \times p3 \quad (6)$$

$$W = 0.6 \times w1 + 0.3 \times w2 + 0.1 \times w3 \quad (7)$$

$$C = 0.5 \times c1 + 0.4 \times c2 + 0.1 \times c3 \quad (8)$$

Table 4. The score of each secondary indicator.

Symbol	Secondary Indicators	Scoring Interval	Final Score for Level 1 Indicators
p1	U ₁₁ :Developed Root System	[90, 100]	P
p2	U ₁₂ : Dense Canopy	[80, 90]	
p3	U ₁₃ :Monodominant communities	[0, 80]	
w1	U ₂₁ : Prop roots	[90, 100]	W
w2	U ₂₂ : Aerial roots	[80, 90]	
w3	U ₂₃ : Air roots	[0, 80]	
c1	U ₃₁ :Aeration and Water Absorption Systems	[90, 100]	C
c2	U ₃₂ : Permeation and Corrosion Protection Systems	[80, 90]	
c3	U ₃₃ : Salt Excretion System	[0, 80]	

Based on the final scores, the distribution of indicators according to importance in this bionic design can be seen in Table 5, which can be of methodological help for further study.

Table 5. Quantification table of importance grading of each indicator.

Risk Class	Name	Range of Quantification
I	Most Important	(80, 100]
II	Moderately important	(50, 80]
III	Least important	(0, 50]

3.2.2. Analysis of Design Elements

According to the calculation, in the mangrove bionic design, the importance of the prototypical features of the design elements is ranked as follows: structure > morphology > system. The design needs to take into consideration the importance distribution of each feature and related elements. According to the secondary weights, the most important aspects of structure are the prop and aerial roots, following is the respiratory roots. The most important elements of morphology are developed root systems and dense canopies, with monodominant communities being the secondary. The systematic aspects acquire poor scores and thus are not considered in this design.

Considering both structural and morphological features, it can be concluded that the well-developed and diverse root system of mangrove plants is the key to this bionic design. The extraction of the root system's critical structural and morphological features should be scientifically feasible, function-oriented, environmentally friendly, and aesthetically beautiful. The features are then transformed and modified to the elements for the design.

3.3. Numerical Simulation Experiments on Disaster Prevention and Mitigation Structures

3.3.1. Introduction to EDEM Software

The Discrete Element Method (DEM) is a material analysis method for discrete particles. EDEM is a modeling software based on DEM that can be used for the simulation and analysis of the process of particles and production of manufacturing equipment in the industrial field. The powerful simulation capabilities of EDEM allow for a reliable simulation of the particles indebris flows particles hitting different groups baffles.

3.3.2. Extraction of the Features of Root Systems

Based on the analysis of the elements in the design, the morphological and structural characteristics of the root system of the mangrove plant are extracted and a linear diagram is drawn accordingly. Taking into consideration the experimental properties of the numerical simulation, the root systems are transformed and simplified into three geometric shapes: square column, round column, and triangular conical column, meanwhile the initial optimization of the traditional baffle groups is conducted to form a new basic structure of baffle groups. The extraction and transformation process is shown in Figure 10.

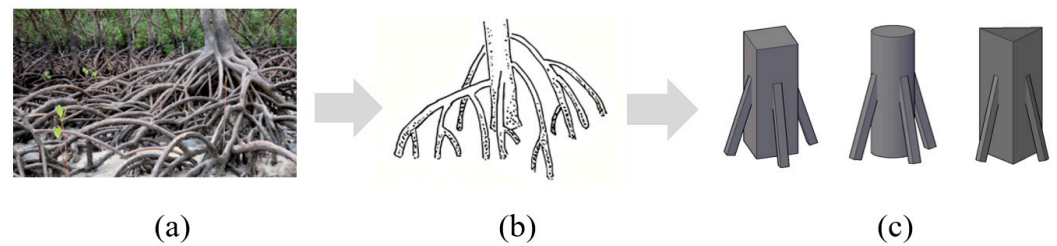


Figure 10. The extraction and transformation of root characteristics of mangrove plants, (a) mangrove root system, (b) linear diagram of root morphology and structure, and (c) geometric structure condensation.

3.3.3. Simulation Device and Test Baffle Group Type

The simulation device refers to the model of previous papers [37,38] and material parameters [39–41]. The test platform consists of five parts: material box, chute, piling platform, side plate of platforms, and blocking baffle groups. The volume of the material box is 0.11 m^3 , the length of the chute is 420 cm, and the inclination angle is 35° , while the platform is 2.5 m by length and 2.5 m by width. The baffle group uses three rows of baffles with a side length of 50 mm, a height of 180 mm, and a blocking distance of 400 mm (the distance from the foot of the chute to the first row of baffles). The row spacing is of 70 mm. The column spacing is 50 mm and 90 mm, respectively. The 3D model is shown in Figure 11.

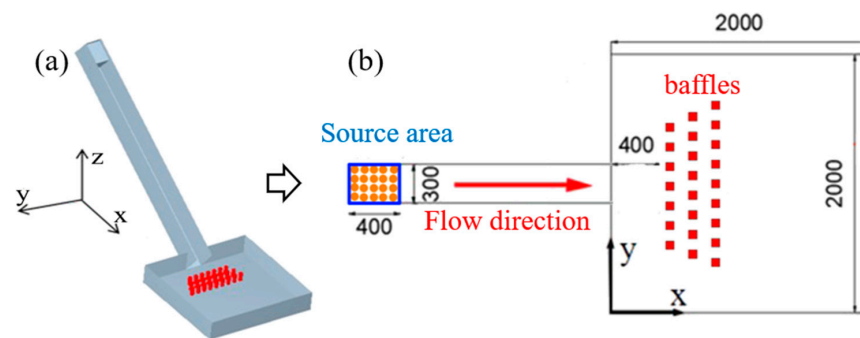


Figure 11. DEM model of debris flow impact baffle group: (a) 3D numerical model; (b) top view of the model.

In order to analyse interception effect of the basic structure of different types of new baffles against the debris flow, in the DEM, a total mass of 60 kg of debris flow particles with a diameter mainly ranging from 5 to 20 mm is simulated, as well as the three new baffles and the three traditional ones. The types of baffle groups involved in the test are shown in Figure 12. Figure 12 shows that the different baffles shapes in numerical investigation. Z1, Z3, and Z5 are conventional baffles, and Z2, Z4, and Z6 are new bundles. A total of 12 sets of tests were set up to numerically simulate each of the six types of banks at two inter-baffle opening distances.

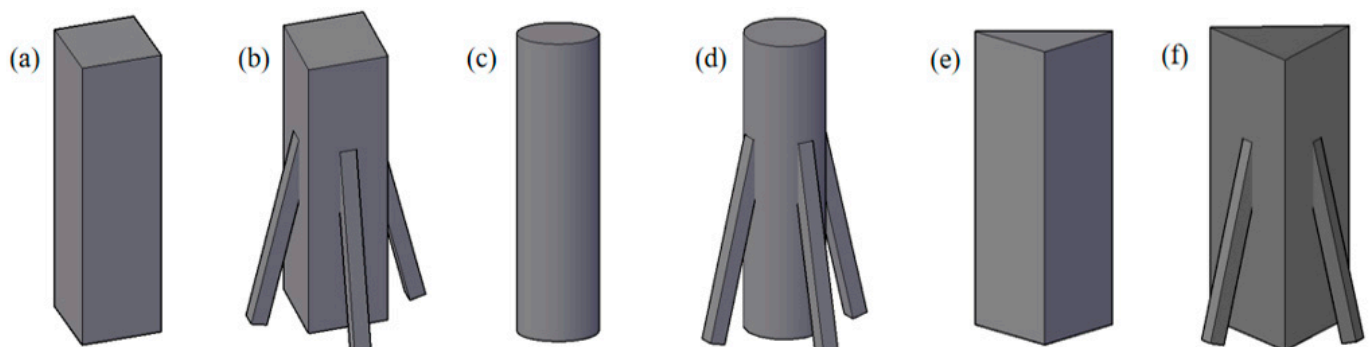


Figure 12. Baffle group type, (a) Z1; (b) Z2; (c) Z3; (d) Z4; (e) Z5; (f) Z6.

3.3.4. Low-Carbon Cement Description

In actual engineering, the building materials for baffles should be low-carbon cement. The materials are shown in Table 6. The development of low-carbon cement will be listed in our future works due to the space limitations. However, in this study, the baffles were constructed by wall element in EDEM for the research convenience. The debris flow prevention efficacy is stressed rather than the baffles' impact resistance performance in this study. To be focused on the efficacy of debris flow prevention, the deposition of the debris flow is to be specially studied instead of the structure.

Table 6. The low-carbon material in this design.

Additive	Description
Shield residue soil	Liquid limit $\leq 25\%$, plastic limit $\leq 15\%$, plasticity index ≤ 10 , liquidity index ≤ 1 , for high water content of low liquid limit clay
Blast furnace slag	Specific surface area of not less than $0.28 \text{ m}^2/\text{g}$, with SiO_2 content $\geq 20\%$ and CaO content $\geq 20\%$
Steel slag	SiO_2 content $\geq 12\%$ and CaO content $\geq 30\%$
Magnesium oxide	The activity of magnesium oxide is in 90 s–100 s
Carbide slag	Powder not less than 200 mesh
Polyacrylamide	Anionic polyacrylamide, molecular weight 8–20 million

Previous studies have listed different kinds of calculation methods for carbon emissions of concrete. Some methods cannot be accurately calculated [42], some methods only calculate the average CO_2 emission amount of such building material industry [43]. The concrete carbon emission calculation based on life cycle assessment have been used in this paper to rapidly and precisely calculate the CO_2 emission [44]. The calculation formula was shown as follows:

$$GHG_{manu} = GHG_{mine} + GHG_{ener} + GHG_{tran}$$

where GHG_{manu} is the carbon emissions for production of unit concrete, GHG_{mine} is the total emission amount in material production process, the CO_2 equivalent; GHG_{ener} is the total emission amount in energy production and application process, the CO_2 equivalent; GHG_{tran} is the total carbon emission amount during transportation of various materials, products and energy, the CO_2 equivalent.

$$GHG_{mine} = \sum_{i=1}^n Q_i F_{GHG,i} \times (1 - \alpha_i)$$

where GHG_{mine} is the total emission amount of GHG in raw material production process, the CO_2 equivalent; Q_i is the consumption of Class i raw material, kg; $F_{GHG,i}$ is the carbon emission factor in Class i raw material production; α_i is the recovery coefficient of class i raw material.

$$GHG_{ener} = \sum_{i=1}^n E_i F_{GHG,i}$$

where, GHG_{ener} is the total emission amount in energy production and application process, the CO_2 equivalent; E_i is the consumption of Class i energy, including fossil energy and electric power; $F_{GHG,i}$ is the carbon emission factor of Class i energy.

$$GHG_{tran} = \sum_{j=1}^m \sum_{i=1}^n Q_{i,j} D_{i,j} F_{GHG,j}$$

where, GHG_{tran} is the total carbon emission amount during transportation of various materials, products and energy, kg; $Q_{i,j}$ is the total amount of Type i material in Type j transportation mode, kg; $D_{i,j}$ is the transportation distance of Type i material in Type j transportation mode, km; $F_{GHG,j}$ is the carbon emission factor of different transportation modes.

The calculation results were shown in Figure 13. The materials used in this study is better than traditional cement in performance of the CO₂ emissions and energy consumption. The low-carbon material show that 75% CO₂ emissions have been reduced when compared with traditional cement. The Figure 13 also shows that the energy consumption of low-carbon material has been reduced by 70% when compared with traditional cement.

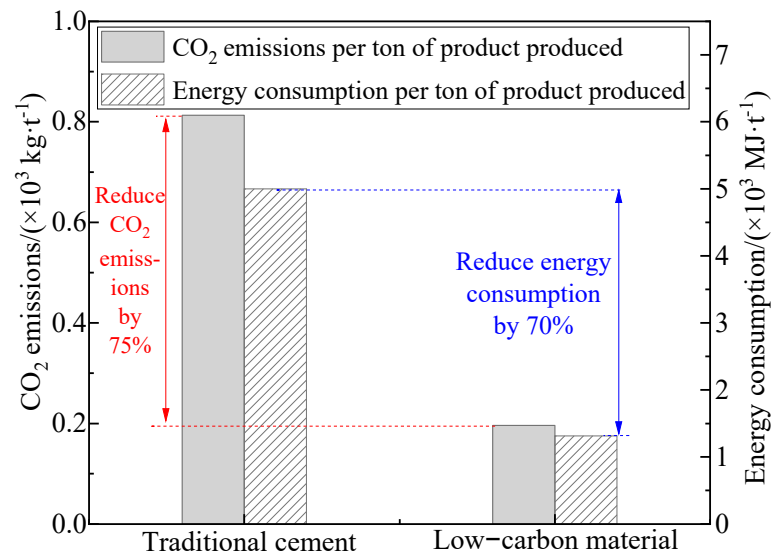


Figure 13. The comparison of CO₂ emissions and energy consumption between traditional cement and low-carbon material.

3.3.5. Parameter Setting

In DEM simulations, the physical parameters of the materials that are required to be calibrated are the intrinsic parameters of the material and the contact parameters between the materials. The intrinsic parameters include the Poisson's ratio, shear modulus, and density, and the contact parameters include the static friction factor, rolling friction factor, and elastic recovery coefficient. The intrinsic and contact parameters of the material in this experiment are set by reference to the previous studies [39–41]. The particles, the chute, the block baffle groups, the area, and the platform side plates are all considered rigid bodies and, thus, the deformation resulting from the particle-particle and particle-steel contact is not considered. Consequently, the elastic recovery coefficients are set identically the same. The static and rolling friction factors between the particles have been measured in previous studies [39]. Ultimately, after several tuning of the numerical simulation parameters, the intrinsic parameters of the material and the contact properties were determined, as shown in Tables 7 and 8.

Table 7. The material intrinsic parameters.

Material	Poisson's Ratio	Density/(kg·m ^{−3})	Shear Modulus/Pa
Debris flow granules	0.25	2100	8×10^8
Chutes (steel)	0.3	7900	7×10^{10}
Baffle groups, baffle areas and side panels	0.3	7900	7×10^{10}

Table 8. The contact properties.

Type of Contact	Elastic Recovery Factor	Coefficient of Static Friction	Rolling Friction Coefficient
Pellets-Pellets	0.6	1.33	0.15
Pellets-Steel	0.6	0.453	0.05

3.3.6. Analysis of Numerical Simulation Results

Process and Velocity Analysis

Figure 14 shows the velocity analysis and stationary accumulation of debris flow particles impacting the Z1 baffle group with a blocking distance of 400 mm and a distance of 90 mm each between. As shown in Figure 14a, when $t = 0$ s, the particles are produced in the DEM, and they are in a stationary accumulation state under the blockage of the material box. When $t = 0.3$ s, the debris flow particles in Figure 14b start to collapse due to the gravity, and a more obvious stratification of the velocity occurs. The particles in the front now have higher velocity while the particles on the far end are still at rest, and this lasts until $t = 1.1$ s, as shown in Figure 14c. In Figure 14d, the frontmost particle rushes to the foot of the slope, and its velocity decreases after hitting the bottom plate of the baffle area, and thus produces the phenomenon of leaping. Due to the obstruction of the front-end particles, the friction increases and the speed of the following particles decreases, starting to slowly slide in the baffle area. Some particles pass through the gap between the baffles, but are then blocked by the following staggered baffle groups. They then accumulate at the stacking area. The particles at the far end are obstructed by the stationary accumulations at the front end and thus disperse to the sides of the original path, as shown in Figure 14e. Eventually, the particles lose kinetic energy to become still in front of the baffle groups. After that, the following particles decelerate and slide on the accumulation until all particles stop moving, as shown in Figure 14f. In summary, the process of debris flow particles impacting the baffle group can be divided into an initiation phase, an acceleration phase, a deceleration phase, and a blocking and accumulation phase.

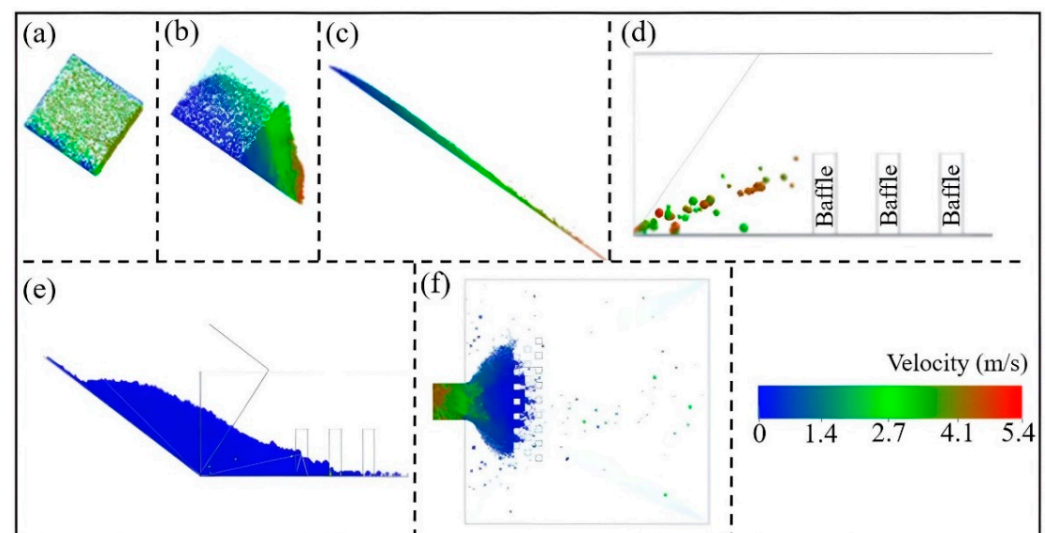


Figure 14. The impact of debris flow particles on a cluster of Z1 baffles: (a) $t = 0$ s; (b) $t = 0.3$ s; (c) $t = 1.1$ s; (d) $t = 1.3$ s; (e) $t = 2$ s; (f) $t = 4$ s.

In order to better grasp the blocking efficiency of different types of baffles on the velocity of debris flow particles, a series of numerical experiments are conducted in this study. Six kinds of baffles with a set baffle distance of 90 mm are tested against the debris flow particles as an example. In Figure 15, before the point $t = 1.3$ s, the maximum velocity of the debris flow, as well as the time required to reach the peak velocity, is almost the same

in all six cases due to the same working conditions. After 1.3 s, the debris flow particles start to be blocked by different blocking baffle groups and the speed decreases by different degrees. The speed of the flow is lower after impacting the Z2, and Z4 baffle groups, than that after impacting Z1, and Z3 baffle groups, respectively. However, after moving the Z5 baffle group, the speed is higher than that after impacting Z6 ones. This indicates that the new baffles of Z2 and Z4 are more effective in reducing the impact velocity of the debris flow than the traditional baffles of Z1 and Z3. However, Z6 does not perform better than Z5.

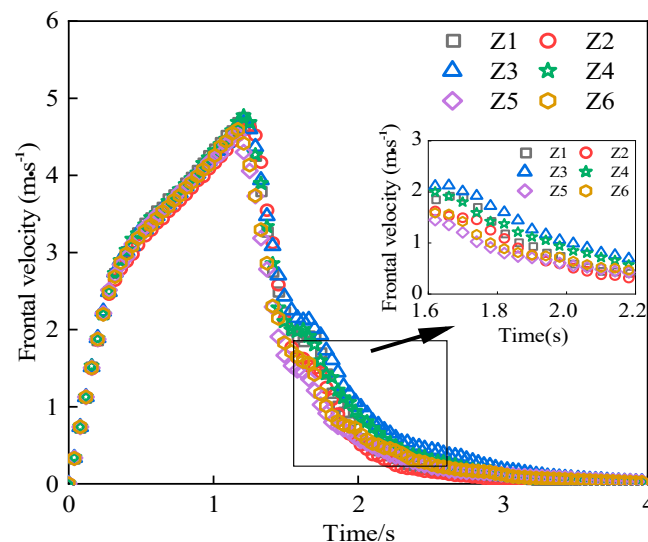


Figure 15. The effect of different baffle groups on the particle tap velocity of debris flows.

Effect of Different Baffle Groups and Inter-Baffle Openings on Particle Accumulation Patterns

In order to investigate the blocking efficiency of different inter-baffle openings on the debris flow, the diagrams of the accumulation area of the particle flow after impacting the same type of baffle group but with different inter-baffle opening distances are drawn as in Figure 16. Figure 16 shows that the accumulation of the debris flow within the three rows of baffles in either of the six cases, whether the distance between baffles is 50 mm or 90 mm. In the cases of the traditional baffle groups, the debris flow accumulates just by the row of baffles, and all rows of are made full use of. However, in the cases of the new baffle groups with a opening distance of 90 mm, the debris flow stops and accumulates before reaching the third row of baffles. This means that the new structure of the baffle groups can better block the debris and only two rows can perfectly achieve the goal. The above phenomenon shows that the six baffle groups with either 50 mm or 90 mm openings can well block the debris flows and the new types of baffles with an opening distance of 90 mm can achieve the function with only the first two rows while the traditional types requires three rows.

According to the analysis of the blocking effect of the baffle type on the debris flow in Figure 17, it can be seen that all baffle types have an excellent blocking effect on the flows. In general, the impact distance and width of the accumulation areas varies little between different types of baffle groups. Figure 16a shows that when the opening distance is of 50 mm, the accumulation areas of Z1, Z2, Z3, Z4, Z5, and Z6 are 628,413, 582,935, 658,281, 586,552, 581,756, and 571,577 mm², respectively. Figure 16b shows that when the opening distance is 90 mm, the accumulation areas of Z1, Z2, Z3, Z4, Z5, and Z6 are 629,691, 559,492, 583,959, 561,273, 665,201 and 611,341 mm², respectively. The comparison shows that the Z2, Z4, and Z6 enable a smaller accumulation area of the debris flows.

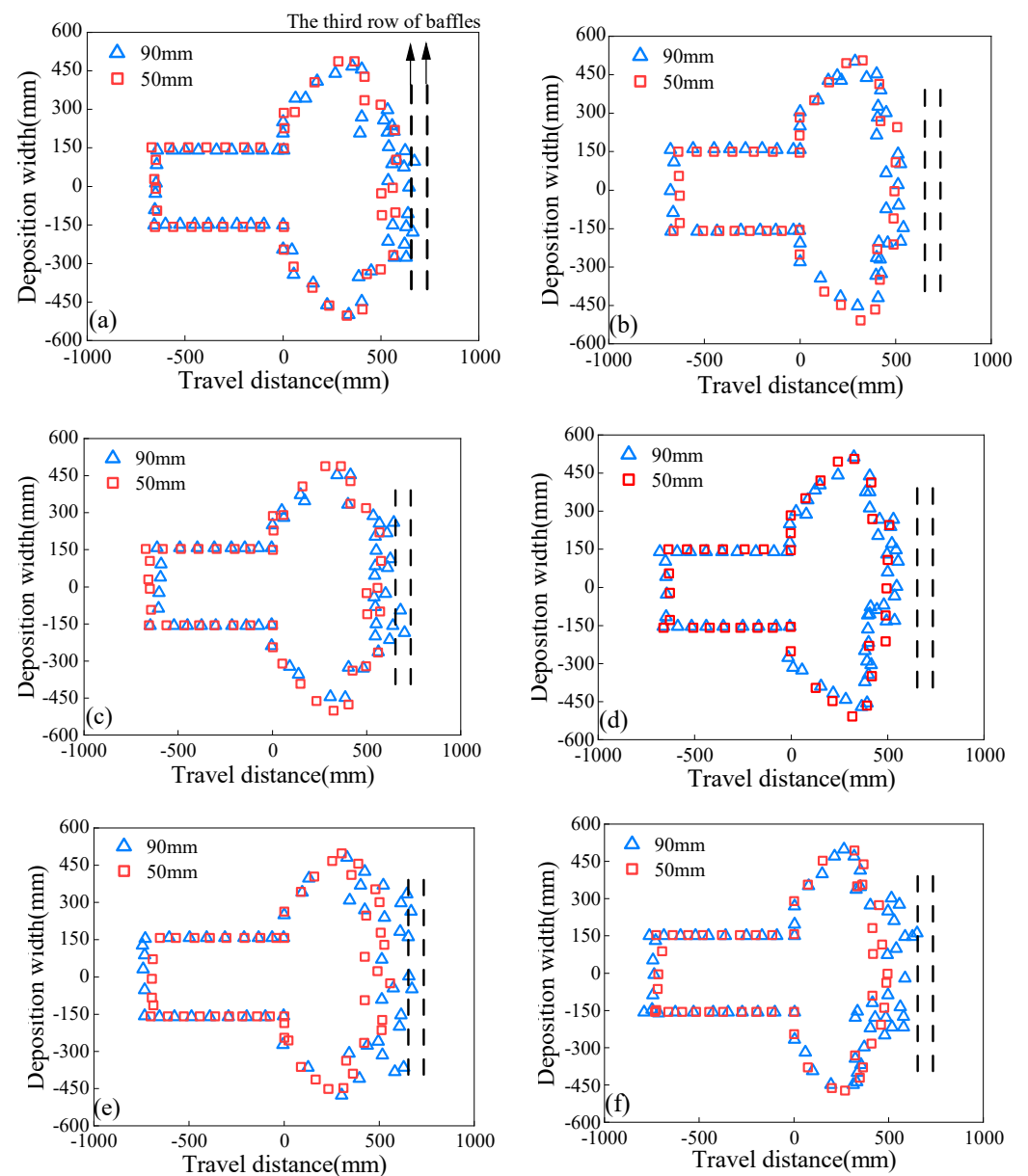


Figure 16. The influence of the distance between baffle openings on the effectiveness of debris flow interception: (a) Z1, (b) Z2, (c) Z3, (d) Z4, (e) Z5, (f) Z6.

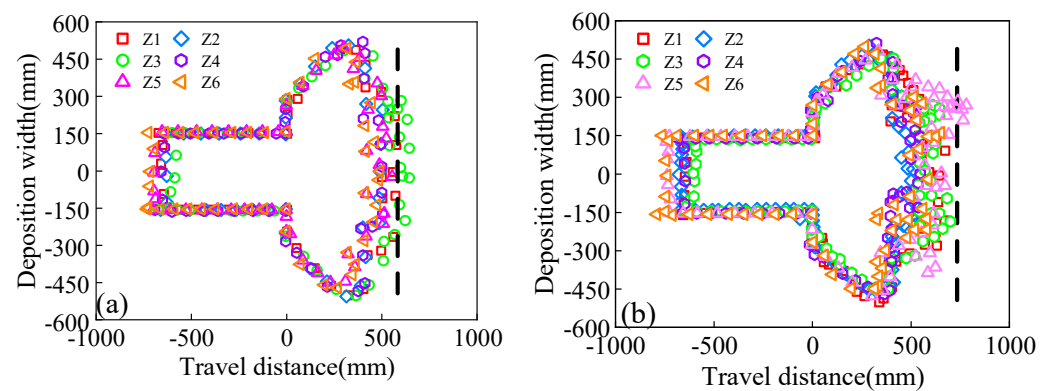


Figure 17. The effect of baffle type on the morphology of the debris flow baffle: (a) 50 mm opening distance between baffles, (b) 90 mm opening distance between baffles.

In order to investigate the influence of the baffle types on the mass distribution of the accumulation areas after the blocking of the debris flow, as shown in Figure 18a, six types of baffle groups with a 90 mm opening are selected, and a zone is set every 80 mm along the slope to acquire the mass of the particles within them and thus to analyse the features of the mass distribution in each cases. The zones are labeled as A1–A10. As seen in Figure 18b, the mass distribution of the debris flow varies little in different cases. The mass all follow the pattern of firstly increasing and then decreasing in all the six cases. Within the 400 mm from the foot of the slope, mass of the accumulation in each zone is higher in the cases of the new baffle groups than that with the traditional ones. The situation reverses when it comes to the areas that are beyond the this 400 mm line. This is because the new baffles have a ‘foot’ that keeps more particles in the front of rather than letting them pass. Among the 6 types, the Z2 and Z4 are with the lowest mass behind the baffles.

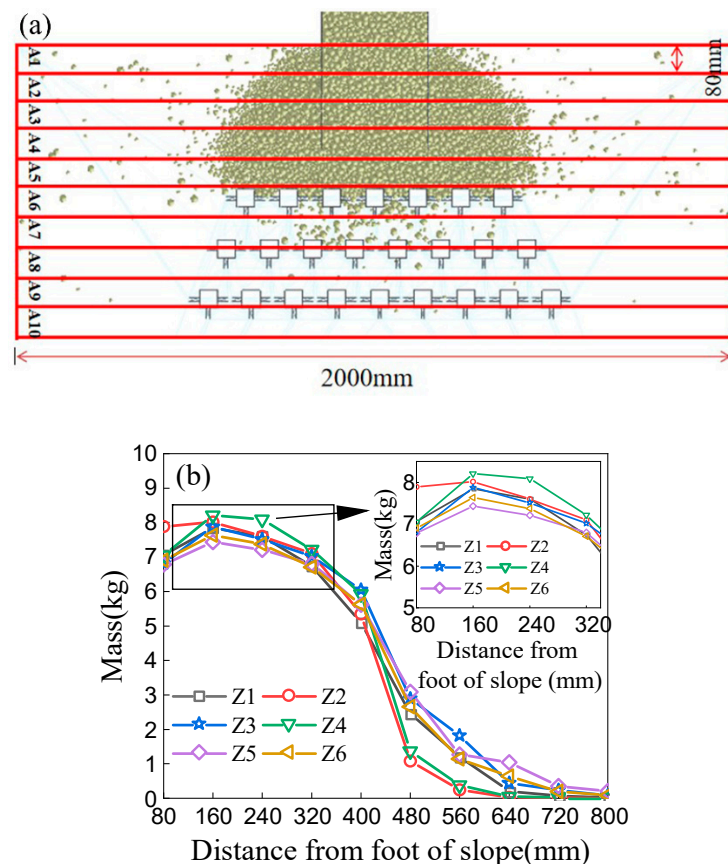


Figure 18. The influence of baffle type on baffle mass distribution: (a) schematic plan of mass calculation in the baffle area, (b) influence of baffle type on mass distribution in the baffle.

3.3.7. Summary

Numerical simulations show that the Z2 and Z4 structures have the best blocking effect, which are the two geometric shapes of square and round columns in the main body, with the addition of a root-like base at the bottom. These two are the structures with the best performance. However, considering the artistic needs and bionic design principles, the round column is more suitable for the design and may achieve a more pleasing appearance. The transformation of the product’s shape is shown in Figure 19.

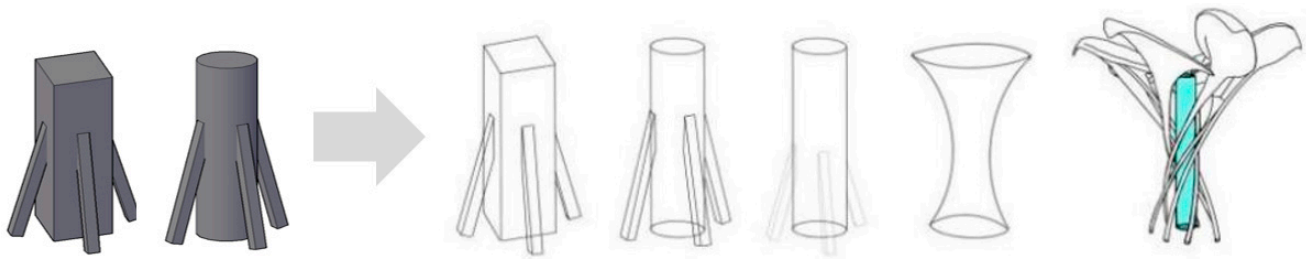


Figure 19. The product shape modification and transformation process.

3.4. Mangrove Bionics-based Design Practice for Disaster Prevention and Structural Mitigation Products

The final design is based on the “Six Elements and Ten Steps” systematic bionic design methodology to level the design requirements. It is a modified version to the existing baffle groups based on a bionic feature of the root and forms of the mangroves. In addition, the aim is to realise the goal of being both effectively wind and wave-resistant as well as visually pleasing. It reflects a harmonious combination of both the beauty of nature reserves and tourist attractions and the artificial projects of prevent and mitigate the natural disasters.

3.4.1. Design on the Appearance Structural Shape

Firstly, two optimal baffle group structures are selected through numerical simulation and this ensures that the structures are scientifically feasible, then the design will be modified according to aesthetic principles. The design is overall a mangrove-like rotating structure with artistic hollowed-out appearance, leaving a impression of being dynamic. Figure 20a is the front view pic. The upper part of the structure is similar to a blooming flower. As shown in the Figure 20b. The lower part of the structure is similar to a root system, which is a geometricalized combination of the structures of several roots including plate, finger-like, knee-shaped, and creeping-snake-shaped ones.

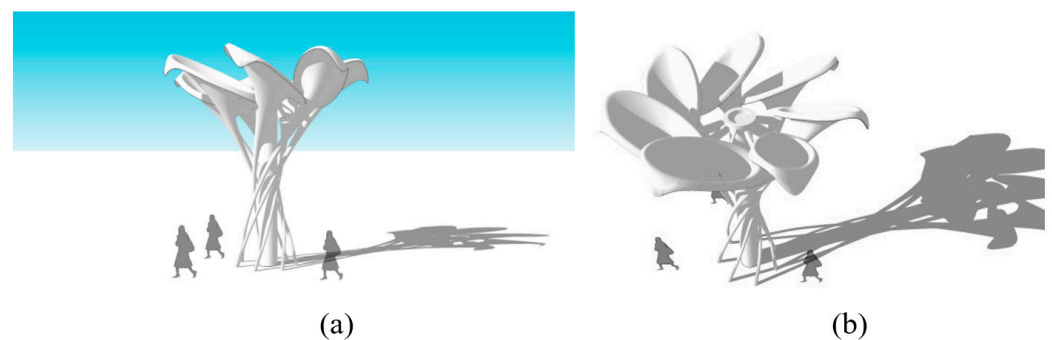


Figure 20. The analysis of product modeling structure characteristics: (a) front view, and (b) top view.

Colour Material

The optimization of the baffle groups’ structure is an aesthetic revision of the previous protective engineering that disturbs nature, and it tries to achieve a harmonious relationship between the environment and the disaster prevention engineerings implemented. The scheme’s aesthetic aspire is shown not only in the form but also in the selected colors and the ecological awareness and sustainable development principles reflected. Considering cement is highly alkaline and has a high carbon footprint, the central column and side pillar feet are replaced with an eco-friendly material, glutinous rice mortar, one of the green high-performance concrete materials. The upper ‘petals’ are made of colored acrylic materials for a clear and fresh texture, and Figure 21a is the daytime view. The edges are lit with spotlights for localized accent lighting to create a colorful ambiance as well as an enchanting and hazy scene during the nightss, and Figure 21b is the night view.



Figure 21. The color and material presentation of products: (a) daytime, and (b) night.

Overall Style

The overall style of new structure is more beautiful than traditional baffles. The traditional baffle is usually simple cylinder or cuboid cement pier (see Figure 2), which is uglily and will destroy the beauty of the scenic spot (Jiuzhai creek or other scenic spots). The artistic is not reflected in the complex structure and color but in the use of simple but unified curves and harmonious colors. The mangrove shape of the main body accompanied by the dynamic design of a blooming flower brings it to the real nature and allows the engineering to live in harmony with the environment.

3.4.2. Functional Design

The scheme is mainly practice-oriented and pays special attention to the diversity of functions. It mainly contains the following three items: the essential function is to set up a effective engineering structure for disaster prevention and mitigation, the secondary goal is to create a dynamic recreation ground, and there is an additional aim to create an Internet celebrity spot for brand marketing.

Effectiveness of Disaster Prevention and Mitigation Protection

The core objective of the mangrove bionic design is to optimize the structure of the blocking baffle group through numerical simulations. With its premise to realize the function of debris prevention, some artistic modifications are also conducted to the simple geometric figures.

Creation of a Dynamic Recreation Ground

The top imitates the dense canopy of mangrove plants. It is also in the shape of a blooming flower petal, which meets the ornamental requirements as well as the needs of visitors to rest at the same time. At night, the illumination of the “petal” edge creates a warm and romantic atmosphere, thus bringing a visual feast to the viewer. The different light intensities, the changes of color, and the shadows well serve the expression of the emotions of the viewers and may provide new ideas for the business model of nature reserves and tourist attractions.

Create an Internet Celebrity Spot

The scheme is of special artistic beauty. In the internet era, it is in line with the trend of the public and has the potential to become an Internet celebrity spot. At the same time, because of its artistic design and applicability, it can be thought-provoking scene for the visitors to reconsider the ecological problems with the idea of sustainable development. On the basis of disaster prevention and structural mitigation products achieving their engineering efficacies, they are encouraged to be designed in harmony with either the nature and the society. It aims to realize a harmony between nature and human, as well as meet the economic goals.

3.4.3. Summary of the Design

The mangrove is not only the key to the realization of the functions but also the inspiration for the appearance. This calls people to reconsider the relationship between nature and human beings. The design has significant advantages over traditional baffle groups in terms of scientific feasibility, functional orientation, environmental protection, as well as aesthetics, and Figure 22 shows the comparison. Creating this new landmark in nature reserves and tourist attractions with the help of anthropomorphic natural shapes, it leaves the visitors a sense of grandeur and the impact on both the eyes and the emotion make it a representative of the harmony between human and nature. This design is a combination of engineering, art and natural environment and may provide a direction for the study of ecological and economic disaster prevention and products.

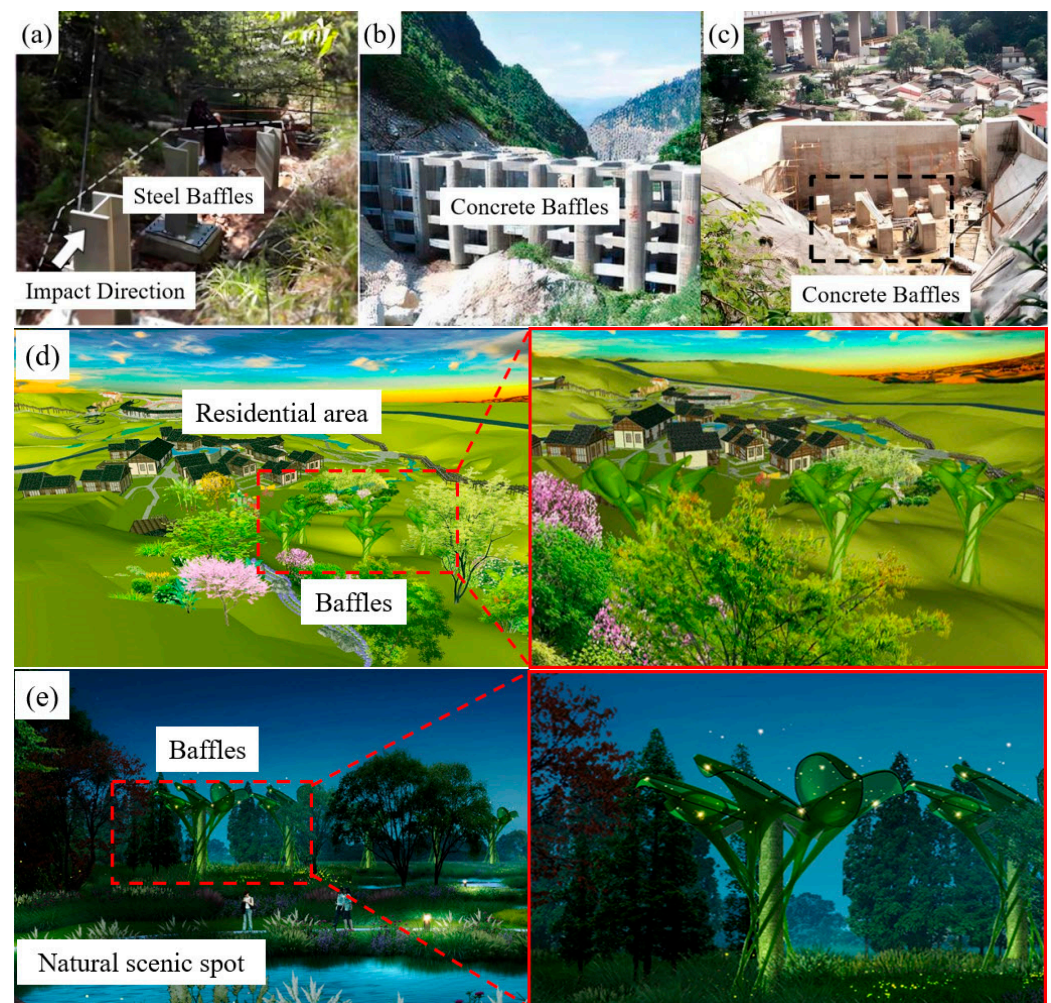


Figure 22. A comparison of traditional baffle group application examples and design renderings, (a) traditional steel baffles in Hongkong, China, (b) traditional concrete baffles in China mainland, (c) traditional concrete baffles in Hongkong, China, (d) daytime effects of Mangrove baffles, and (e) night effects of Mangrove baffles.

4. Discussion

This paper proposes a bionic engineering-based product design methodology, namely the “Six Elements and Ten Steps” product bionic design methodology, based on the bionic design of mangrove forests for disaster prevention and mitigation. By analyzing and comparing the correlation strength between the six elements of the bionic prototype, namely form, structure, texture, color, function and system, and its performance to achieve the target, the key elements are extracted and the features are refined by the analytic

hierarchy process (AHP), so as to complete the construction of the core function structure model. Through numerical simulation and other scientific experiments, the effectiveness of each model is tested, analyzed and compared, and the optimal model is selected and optimized to shape the product. According to the project requirements, with specific design principles to improve the product of other functional items, feature presentation and other aspects, and finally complete the product design scheme. Based on the results, the following conclusions can be drawn:

- (1) The design of disaster prevention and mitigation products based on mangrove bionics starts from environmental integration and takes functional orientation as the core. Its functional advantages are mainly reflected in the basic functions of disaster prevention and mitigation, and at the same time, it focuses on creating secondary functional items of dynamic recreation space and creating added value of Internet celebrity scenic spots brand marketing. At the same time, the program gives consideration to the aesthetic nature of art, and uses mathematical models and experiments to run through the scientific feasibility, so as to effectively alleviate the problems of hindrance, ornamental and environmental protection in the existing disaster prevention and reduction projects, and achieve the purpose of optimizing the disaster prevention and reduction projects. Finally achieve the purpose of optimizing disaster prevention and mitigation engineering. In addition, it is proposed that the integration of “engineering”, “design”, “ecology” and “business” four elements to form a value chain is the future trend of engineering bionic product design development. It is expected to achieve a win-win situation of social value, ecological value, economic value and artistic value. This product verifies the feasibility of the “six elements and ten steps” product bionic design methodology, and also provides a certain reference for other related design practices.
- (2) The “Six Elements and Ten Steps” product bionic design methodology is based on the perspective of bionic engineering. Aiming at some drawbacks of traditional engineering project design, it tries to put forward a set of design theoretical framework in the form of methodology. The methodology defines the elements and specific steps to be considered in the process of engineering bionic design, and helps designers to efficiently select the key elements of bionic design and its detailed features, namely design elements. Meanwhile, it emphasizes the importance of participating in the evaluation and comparison of scientific experiments, which has strong scientific feasibility and universality of practical application. The interpretation and judgment of product design based on bionic engineering and the corresponding design strategy will vary greatly due to the differences in different engineering application fields, different designers and different periods. Although there are still some limitations in the universality of the application of this design methodology in different engineering fields, it can provide beneficial theoretical support for most benign bionic design innovation.
- (3) The pile group structure designed based on mangrove bionics has better energy dissipation characteristics of debris flow than the traditional pile group structure. The pile mass of particles after the pile can be effectively reduced by 2–3 times, and the pile area and head speed of debris flow can be reduced to varying degrees. The product has guiding significance to the application of disaster prevention and reduction in practical engineering. Compared with the traditional pile group, the structure is more beautiful and has the function of disaster prevention and reduction, which is suitable for laying in the scenic spot.

Author Contributions: Data curation, Y.-Z.B. and X.-Y.W.; funding acquisition, D.-P.W. and Y.-Z.B.; investigation, Y.-Z.B., D.-P.W. and X.-Y.W.; supervision, D.-P.W. and B.Z.; writing, Y.-Z.B., X.-Y.W., Z.-F.L. and M.L. All authors have read and agreed to the published version of the manuscript.

Funding: This research is funded by the State Key Laboratory of Geohazard Prevention and Geoenvironment Protection Independent Research Project (SKLGP2021Z001), Transportation Technology Project of Sichuan Province (2021-A-04), Scientific Research Foundation of Graduate School of Southeast University (Grant No. YBJJ 1844), Postgraduate Research & Practice Innovation Program of Jiangsu Province (Grant No. KYCX17_0130), CAS Original Innovation Program (Grant No. ZDBS-LY-DQC039).

Institutional Review Board Statement: Not applicable for studies not involving humans or animals.

Informed Consent Statement: Not applicable for studies. Not involving humans.

Data Availability Statement: The data that support the findings of this study are available from the first author, Yu-Zhang Bi, upon reasonable request.

Acknowledgments: We wish to thank the anonymous referee for their careful reading and for providing insightful comments to improve the initial version of this paper.

Conflicts of Interest: The authors declare no conflict of interest.

References

- Kabir, M.; Abolfathi, M.; Hajimoradloo, A.; Zahedi, S.; Kathiresan, K.; Goli, S. Effect of mangroves on distribution, diversity and abundance of molluscs in mangrove ecosystem: A review. *Aquac. Aquar. Conserv. Legis.* **2014**, *7*, 286–300.
- Rasmeemasuang, T.; Sasaki, J. Wave reduction in mangrove forests: General information and case study in Thailand. In *Handbook of Coastal Disaster Mitigation for Engineers and Planners*; Butterworth-Heinemann: Waltham, MA, USA, 2015; pp. 511–535.
- Han, M.; Hou, J.; Wu, L. Potential impacts of sea-level rise on China's coastal environment and cities: A national assessment. *J. Coast. Res.* **1995**, *14*, 79–95.
- Sheth, A.; Sanyal, S.; Jaiswal, A.; Gandhi, P. Effects of the December 2004 Indian Ocean tsunami on the Indian mainland. *Earthq. Spectra* **2006**, *22*, 435–473. [[CrossRef](#)]
- McIvor, A.L.; Möller, I.; Spencer, T.; Spalding, M. *Reduction of Wind and Swell Waves by Mangroves*; Working Paper 40; Natural Coastal Protection Series: Report 1; Cambridge Coastal Research Unit: Cambridge, UK, 2012; ISSN 2050-7941.
- Zhou, G. *The Mechanisms of Debris Flow*; Hong Kong University of Science and Technology: Hong Kong, China, 2010.
- Chen, Z.; He, S.; Shen, W.; Wang, D. Effects of defense-structure system for bridge piers on two-phase debris flow wakes. *Acta Geotech.* **2022**, *17*, 1645–1665. [[CrossRef](#)]
- Liu, W.; He, S. Simulation of two-phase debris flow scouring bridge pier. *J. Mt. Sci.* **2017**, *14*, 2168–2181. [[CrossRef](#)]
- Liu, W.; Hu, Y.-X.; He, S.-M.; Zhou, J.-W.; Chen, K.-T. A Numerical Study of the Critical Threshold for Landslide Dam Formation Considering Landslide and River Dynamics. *Front. Earth Sci.* **2021**, *9*, 651887. [[CrossRef](#)]
- Chen, Z.; He, S.; Nicollier, T.; Amman, L.; Badoux, A.; Rickenmann, D. Finite element modelling of the Swiss plate geophone bedload monitoring system. *J. Hydraul. Res.* **2022**, *60*, 792–810. [[CrossRef](#)]
- Yan, S.; Wang, Y.; Wang, D.; He, S. Application of EPS geofoam in rockfall galleries: Insights from large-scale experiments and FDEM simulations. *Geotext. Geomembr.* **2022**, *50*, 677–693. [[CrossRef](#)]
- Jonkman, S.N. Global perspectives on loss of human life caused by floods. *Nat. Hazards* **2005**, *34*, 151–175. [[CrossRef](#)]
- Bi, Y.-Z.; He, S.-M.; Du, Y.-J.; Shan, J.; Yan, S.-X.; Wang, D.-P.; Sun, X.-P. Numerical investigation of effects of “baffles-deceleration strip” hybrid system on rock avalanches. *J. Mt. Sci.* **2019**, *16*, 414–427. [[CrossRef](#)]
- Bi, Y.-Z.; Wang, D.-P.; Fu, X.-L.; Lin, Y.-X.; Sun, X.-P.; Jiang, Z.-Y. Optimal array layout of cylindrical baffles to reduce energy of rock avalanche. *J. Mt. Sci.* **2022**, *19*, 493–512. [[CrossRef](#)]
- Zhang, B.; Huang, Y. Numerical and analytical analyses of the impact of monodisperse and bidisperse granular flows on a baffle structure. *Landslides* **2022**, *19*, 2629–2651. [[CrossRef](#)]
- Zhang, B.; Huang, Y. Impact behaviour of dry granular flow against baffle structure: Coupled effect of Froude and particle characteristics. *Géotechnique* **2022**. under review. [[CrossRef](#)]
- Angeli, M.G.; Pasuto, A.; Silvano, S. Towards the definition of slope instability behaviour in the Alverà mudslide (Cortina d'Ampezzo, Italy). *Geomorphology* **1999**, *30*, 201–211. [[CrossRef](#)]
- Murthy, V.N.S. *Geotechnical Engineering: Principles and Practices of Soil Mechanics and Foundation Engineering*; CRC Press: Boca Raton, FL, USA, 2002.
- Akhlaghi, E.; Babarsad, M.S.; Derikvand, E.; Abedini, M. Assessment the effects of different parameters to rate scour around single piers and pile groups: A review. *Arch. Comput. Methods Eng.* **2020**, *27*, 183–197. [[CrossRef](#)]
- Ng, C.W.W.; Choi, C.E.; Song, D.; Kwan, J.H.S.; Koo, R.C.H.; Shiu, H.Y.K.; Ho, K.K.S. Physical modeling of baffles influence on landslide debris mobility. *Landslides* **2015**, *12*, 1–18. [[CrossRef](#)]
- Bi, Y.; Sun, X.; Zhao, H.; Li, Q.; He, K.; Zhou, R.; Ji, W. Comparison regarding the effects of different baffle systems as impacted by rock avalanches. *Int. J. Civ. Eng.* **2021**, *19*, 127–144. [[CrossRef](#)]

22. Chen, X.-Q.; Chen, J.-G.; Cui, P.; You, Y.; Hu, K.-H.; Yang, Z.-J.; Zhang, W.-F.; Li, X.-P.; Wu, Y. Assessment of prospective hazards resulting from the 2017 earthquake at the world heritage site Jiuzhaigou Valley, Sichuan, China. *J. Mt. Sci.* **2018**, *15*, 779–792. [\[CrossRef\]](#)
23. Jia, Z. Analysis and countermeasures for highway cuts design in harmony with environment. In Proceedings of the 2010 International Conference on Mechanic Automation and Control Engineering, Wuhan, China, 26–28 June 2010; IEEE: New York, NY, USA, 2010; pp. 4225–4228.
24. Junior, W.K.; Guanabara, A.S. Methodology for product design based on the study of bionics. *Mater. Des.* **2005**, *26*, 149–155. [\[CrossRef\]](#)
25. Roth, R.R. The foundation of bionics. *Perspect. Biol. Med.* **1983**, *26*, 229–242. [\[CrossRef\]](#)
26. Yuan, Y.; Yu, X.; Yang, X.; Xiao, Y.; Xiang, B.; Wang, Y. Bionic building energy efficiency and bionic green architecture: A review. *Renew. Sustain. Energy Rev.* **2017**, *74*, 771–787. [\[CrossRef\]](#)
27. Connolly, C. Prosthetic hands from touch bionics. *Ind. Robot. Int. J.* **2008**, *35*, 290–293. [\[CrossRef\]](#)
28. Ren, L.Q.; Liang, Y.H. Preliminary studies on the basic factors of bionics. *Sci. China Technol. Sci.* **2014**, *57*, 520–530. [\[CrossRef\]](#)
29. Palakvangsa-Na-Ayudhya, S.; Pongchandaj, S.; Kriangsakdachai, S.; Sunthornwutthikrai, K. KeptAom: Savings management system to increase long term savings behavior of children. In Proceedings of the TENCON 2017-2017 IEEE Region 10 Conference, Penang, Malaysia, 5–8 November 2017; IEEE: New York, NY, USA, 2017; pp. 2247–2252.
30. Singh, R. Biomimicry: Learning from nature. *J. Eng. Sci.* **2020**, *11*, 533–547.
31. Du, Z.; Yan, Z.; Huang, T.; Bai, O.; Huang, Q.; Han, B. Mechanical design with experimental verification of a lightweight exoskeleton chair. *J. Bionic Eng.* **2021**, *18*, 319–332. [\[CrossRef\]](#)
32. King, S.; Chang, K. *Understanding Industrial Design: Principles for UX and Interaction Design*; O'Reilly Media, Inc.: Sebastopol, CA, USA, 2016.
33. Escande, C.; Chettibi, T.; Merzouki, R.; Coelen, V.; Pathak, P.M. Kinematic calibration of a multisection bionic manipulator. *IEEE/ASME Trans. Mechatron.* **2014**, *20*, 663–674. [\[CrossRef\]](#)
34. Pawlyn, M. *Biomimicry in Architecture*; Routledge: Abingdon, UK, 2019.
35. Kulzhanova, B.; Ongdassynkyzy, D.; Ongdassynova, K.; Duisenbay, A.; Chaimerden, T.; Paromova, Y.; Petrova, Y. Biomimetics—A Hint of Future Technologies in Nature. *J. Biomim. Biomater. Biomed. Eng.* **2021**, *53*, 59–66. [\[CrossRef\]](#)
36. Aryee, P. *30 Animals That Made Us Smarter: Stories of the Natural World That Inspired Human Ingenuity*; Island Press: Washington, DC, USA, 2022.
37. Li, X.; Jiang, L.; Liu, X.; Dang, R.; Liu, F.; Wei, W.; Zhang, T.; Wang, G. Modeling and implementation of a novel amphibious robot with multimode motion. *Ind. Robot. Int. J. Robot. Res. Appl.* **2022**, *49*, 947–961. [\[CrossRef\]](#)
38. Chowdhury, H.; Loganathan, B. Biomimetics of boxfish: Designing an aerodynamically efficient passenger car. In *Biomimicry for Aerospace*; Elsevier: Amsterdam, The Netherlands, 2022; pp. 211–235.
39. Wang, D.; Li, Q.; Bi, Y.; He, S. Effects of new baffles system under the impact of rock avalanches. *Eng. Geol.* **2020**, *264*, 105261. [\[CrossRef\]](#)
40. Wang, D.; Bi, Y.; Li, Q.; He, S. Kinetic response analysis of different types of baffle submitted to rock avalanches based on discrete element method. *Environ. Earth Sci.* **2021**, *80*, 600. [\[CrossRef\]](#)
41. Chen, G.; Han, P.; Wang, Y.; Tian, S.; Qiu, H. Discrete element simulation of retaining effect of retaining piles on debris flow of landslide. *J. Railw. Sci. Eng.* **2022**, *19*, 129–140. (In Chinese) [\[CrossRef\]](#)
42. Van Der Werf, G.R.; Randerson, J.T.; Collatz, G.J.; Giglio, L. Carbon emissions from fires in tropical and subtropical ecosystems. *Glob. Chang. Biol.* **2003**, *9*, 547–562. [\[CrossRef\]](#)
43. Shen, W.; Cao, L.; Li, Q.; Zhang, W.; Wang, G.; Li, C. Quantifying CO₂ emissions from China's cement industry. *Renew. Sustain. Energy Rev.* **2015**, *50*, 1004–1012. [\[CrossRef\]](#)
44. Zhao, C.Z.; Liu, Y.; Ren, S.W.; Quan, J. Study on carbon emission calculation method of concrete. *Key Eng. Mater.* **2018**, *768*, 293–305. [\[CrossRef\]](#)

Disclaimer/Publisher's Note: The statements, opinions and data contained in all publications are solely those of the individual author(s) and contributor(s) and not of MDPI and/or the editor(s). MDPI and/or the editor(s) disclaim responsibility for any injury to people or property resulting from any ideas, methods, instructions or products referred to in the content.